

Article

Laser Sealing for Vacuum Plate Glass with PbO-TiO₂-SiO₂-R_xO_y Solder

Hong Miao ^{1,*}, Lingcong Zhang ¹, Sixing Liu ¹, Shanwen Zhang ^{1,*}, Saim Memon ²  and Bi Zhu ¹

¹ College of Mechanical Engineering, Yangzhou University, Yangzhou 225127, China; zlc121305139@163.com (L.Z.); meesxliu@163.com (S.L.); mengxiangba@163.com (B.Z.)

² London Centre for Energy Engineering, School of Engineering, London South Bank University, London SE1 0AA, UK; s.memon@lsbu.ac.uk

* Correspondence: mh0514@163.com (H.M.); swzhang@yzu.edu.cn (S.Z.); Tel.: +86-138-5270-6878 (H.M.); +86-183-6131-7675 (S.Z.)

Received: 24 February 2020; Accepted: 9 April 2020; Published: 13 April 2020



Abstract: Laser sealing for vacuum plate glass is a key step in developing the cost-effective smart vacuum-glass window for the drive towards net-zero energy buildings. In this paper, the pores, cracks, and interface with laser welding are analyzed in depth using PbO-TiO₂-SiO₂-R_xO_y system sealing solder to prepare vacuum flat glass. The microstructure of the sealing layer was analyzed by a BX41M-LED metallographic microscope, and the interfacial bonding characteristics were observed by thermal field emission scanning electron microscopy (SEM). The solder was analyzed by an energy spectrometer, and the influence of laser power, sealing temperature, and sealing speed on the gas holes and the crack and interface separation of the sealing layer are reported. The results show that when the laser power reached 80 W at the welding speed of 2 mm/s, the bulk solder disappeared to most of the quantity and the sealing surface density was higher, due to which negligible pores and micro cracks were found. Thus, the sealing quality of the sealing layer is considered to be suitable when the temperature of 470 °C was maintained and the solder has 68.93% of Pb and 3.04% Si in the atom fraction to achieve the wet the glass substrate surface whilst improving the bonding quality.

Keywords: laser sealing; vacuum plate glass; sealing layer; pore; crack; interface separation; solder glass

1. Introduction

Vacuum plate glass, as a new type of transparent energy-saving advanced insulation technology currently emerging in the world, has excellent insulation, anti-aging, and infrared reflection properties. It has wider scope in the net-zero energy buildings due to its lower U-value of less than 1 Wm⁻²K⁻¹ [1,2] for vacuum-separated glass sheets and 0.33 Wm⁻²K⁻¹ for dual-vacuum-separated three glass sheets [3,4]. It is a research hotspot in glass processing technology in China and worldwide. Laser welding has the advantages of small heat input, high energy density, a narrow heat affected zone, large penetration, and small thermal deformation [5], so it has wider application prospects and is considered one of the most advanced welding methods in the 21st century [6–10].

At present, studies on sealing materials and sealing performance are mainly focused in glass-manufacturing industries. Miao et al [11] studied the properties of vacuum plate glass for sealing; Zhang et al [12] studied the formation mechanism of sealing edge pores for vacuum glazing using the laser brazing technique. Zhang et al [13] studied the influence of welding process parameters on the pores' formation in pulsed laser-welded vacuum plate glazing. For the porosity, crack, and interface separation of the sealing layer, the sealing effect can also be judged according to the

visual inspection, but there is no deep theoretical research on the bonding performance of the sealing solder and the glass matrix [14].

In this paper, the experimental study and analysis of laser welding parameters and microscopic observation results are carried out for porosity, crack, and interface failure caused by laser sealing. It is found by field emission scanning electron microscopy (SEM) that the advantages of using PbO-TiO₂-SiO₂-R_xO_y as sealing solder are that it has good wettability with soda lime glass and the thermal expansion coefficient of the two is similar. The disadvantages are that it has poor temperature control accuracy under sintering conditions, and it is easy to produce defects such as pores and cracks. However, the sealing can be fully utilized under laser sealing conditions. The vacuum flat glass was made by welding. The welding condition and using temperature of the sealing solder were obtained by sintering test at different temperature and power. The average grain size of the solder was ensured by mechanical method. The microstructure of the sealing layer was analyzed by a BX41M-LED metallographic microscope. The interfacial bonding characteristics were observed by thermal field emission scanning electron microscopy (SEM). The solder was analyzed by energy spectrometer [15]. The above tests will provide the basis for the optimization of sealing temperature parameters, service life prediction and structural improvement design, improve the sealing reliability of vacuum plate glass, and lay a foundation for manufacturing and industrialization.

2. Materials and Methods

2.1. The Testing Materials

The two soda-lime glass sheets' dimensions of 30.0 mm × 30.0 mm × 4.0 mm are used in the experiments. Based on the principle of equal thickness interference, the elastic modulus of the glass is measured. The air film wedge is formed on the upper surface of the standard plate glass and the lower surface of the plate glass to be measured. The distribution of the equal thickness interference fringes of the plate glass are to be measured under natural and stress conditions, respectively, and the elastic modulus of the glass is 72.45 MPa, the Poisson's ratio is 0.22, tensile strength is 40 MPa, compressive strength is 880 MPa (the tensile and compressive strength are selected according to the lower limit), PbO-TiO₂-SiO₂-R_xO_y powder is used as the solder, and the composition and the indicators are shown in Table 1.

Table 1. Composition and performance of the filler alloys.

Composition	wt%	Basic Performance Index	
PbO	75	Sealing temperature/°C	420~520
TiO ₂	15		
SiO ₂	10	Coefficient of thermal expansion/°C ⁻¹	90~94 × 10 ⁻⁷
CuO	<2.5		
Fe ₂ O ₃	<2.5	Melting temperature/°C min ⁻¹	460~480

The PbO, TiO₂, SiO₂, CuO, and Fe₂O₃ powders were mixed evenly according to a certain mass fraction and were then put into the stainless steel ball mill and mixed with a certain amount of dispersant. The control of particle size was achieved through the adjustment of the ball mill mesh, feed volume, the number of steel balls, steel ball size ratio, ball mill speed, and other variables. PbO-TiO₂-SiO₂-R_xO_y solder with a particle size range of 1~25 μm was obtained, and the average particle size was guaranteed to be 12.15 μm. Figure 1 shows the SEM diagram of the encapsulated solder powder. The cylindrical solder for the experiment was obtained by pressing for 12 min under 8 MPa pressure with a powder press, and the particle size was 30 μm.

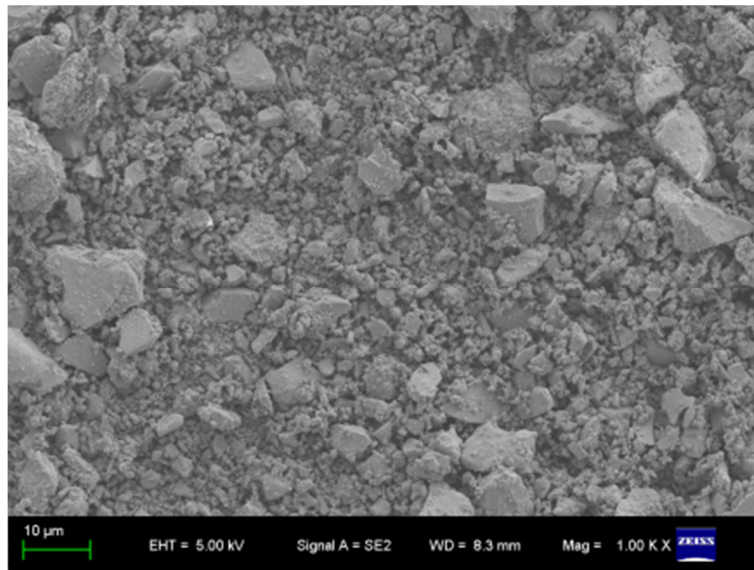


Figure 1. Scanning electron microscopic (SEM) image of the encapsulated solder powder made of $\text{PbO-TiO}_2\text{-SiO}_2\text{-R}_x\text{O}_y$. (Hitachi Manufacturing Co., Ltd., Tokyo, Japan).

2.2. Experimental Testing Methodology

An ultrasonic cleaning machine is needed to clean the glass before performing these experiments, and a large amount of dust, oxides, oil stains, and other pollutants on the glass surface are removed. First, clean the glass at room temperature for about 10 min, and wipe the glass with anhydrous ethanol and dry it. Then, the first flat glass is laid flat, then the cylindrical solder, as shown in Figure 2, is placed on the surface of the first plate glass, the second plate glass is placed flat on the first plate glass, and the final two pieces of glass are pressed together. With digital display, the heating plate (model: C - MAGHP4) heats the vacuum glass to $280\text{ }^\circ\text{C}$ (the maximum temperature is $500\text{ }^\circ\text{C}$) and insulation occurs for about 10 min, completing the preheating treatment. Finally, the vacuum flat glass sample was placed on the fiber laser platform, and different laser process parameters were selected for experimental study. The following parameters are selected: vacuum is 10^{-3} Pa , laser power is 70 W, welding speed is 2 mm/s, and defocus is -2 mm .

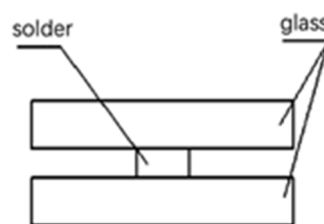


Figure 2. Schematic diagram of the laser-irradiated solder-clad glass.

Next, a small piece of $20.0\text{ mm} \times 20.0\text{ mm} \times 8.2\text{ mm}$ sample is cut from the edge of the sealed vacuum plate glass by the diamond wire saw cutter, of Nanjing University of Aeronautics and Astronautics, in order to remove the oil and other impurities. Firstly, ultrasonic cleaning is carried out in acetone for 15 min, then repeated washing with alcohol, and finally the sample is blow dried. Using an s-4800 thermal field emission scanning electron microscope (SEM) [16], the interface between the solder and glass matrix is combined. The maximum magnification is 8.0×10^5 times and the resolution is 1.0 nm. Using the D8 advanced polycrystalline X-ray diffractometer of Yangzhou University Test Center, the cross-section structure of the solder and the phase structure of the sealing

layer were analyzed. The porosity and distribution characteristics were observed under a bx41m-led metallographic microscope.

3. Results and Discussion

3.1. Formation Mechanism of Pores in Vacuum Glass Sealing Layer by Laser Seal

In this paper, the vacuum laser sealing method is used to test the deposited glass, which belongs to the field of powder sintering in a vacuum environment. At present, the origin of pores and cracks in powder sintering in a vacuum environment mainly includes: residual gas between powder particles or on the surface of matrix, volatilization of impurities, and the size and distribution of the solder particles [17–20]. Because the sealing temperature of the solder is not enough, the pores cannot overflow from the melting layer, and the viscosity of the solder decreases, which leads to a large number of blocky structures. Due to the improper laser sealing conditions, the pores are easy to appear in the sealing layer [21], and the particles centered on the pores extend outwards in the form of emission, so the micro cracks with different growth degrees are formed, and the overall extension ability of the cracks is very strong. When the solder particles are smaller but the particles are scattered unevenly or agglomerated, it will also form a large stress concentration in the micro area, and even produce micro crack defects.

Figure 3 shows the microstructure of 70-W, 80-W, and 90-W laser power, respectively. The laser power directly affects the temperature gradient, cooling rate, and the stability of the welding process of the sealing layer, so it has different effects on the pores and cracks in the sealing layer. As shown in Figure 3a, when the sealing power is 70 W, it can be seen that there are many large-diameter pores in the sealing layer, and the distribution is centralized, and the hole depth is obvious. Due to the incomplete melting of the solder, less liquid phase, and higher melt viscosity, the sealing surface is uneven and the stress between solder particles is concentrated, so there are rough cracks of different lengths.

With the increase in laser power, the sealing temperature increases. At 80 W, there is basically no air hole, the sealing layer is flat, and the block structure disappears, as shown in Figure 3b. At this time, the laser temperature can melt the solder, increase the number of molten metal phase, reduce the solder viscosity, and the stress distribution between solder particles is slightly uniform. At the same time, with the increase in laser power, the wettability of the molten powder is enhanced, which is conducive to the diffusion of the powder, the crack of the sealing layer is obviously shortened, and the sealing quality is improved.

When the laser power reaches 90 W, there are still some defects on the surface of the sealing layer. The surface is not smooth, but the defects are relatively small. As shown in Figure 3c, this is because the viscosity of the molten solder becomes very low, the solder converges with the increase of temperature, the molten solder is burned, and the sealing layer is no longer flat. It can be seen that the laser power is 80 W, and the sealing quality of the sealing layer is the best.

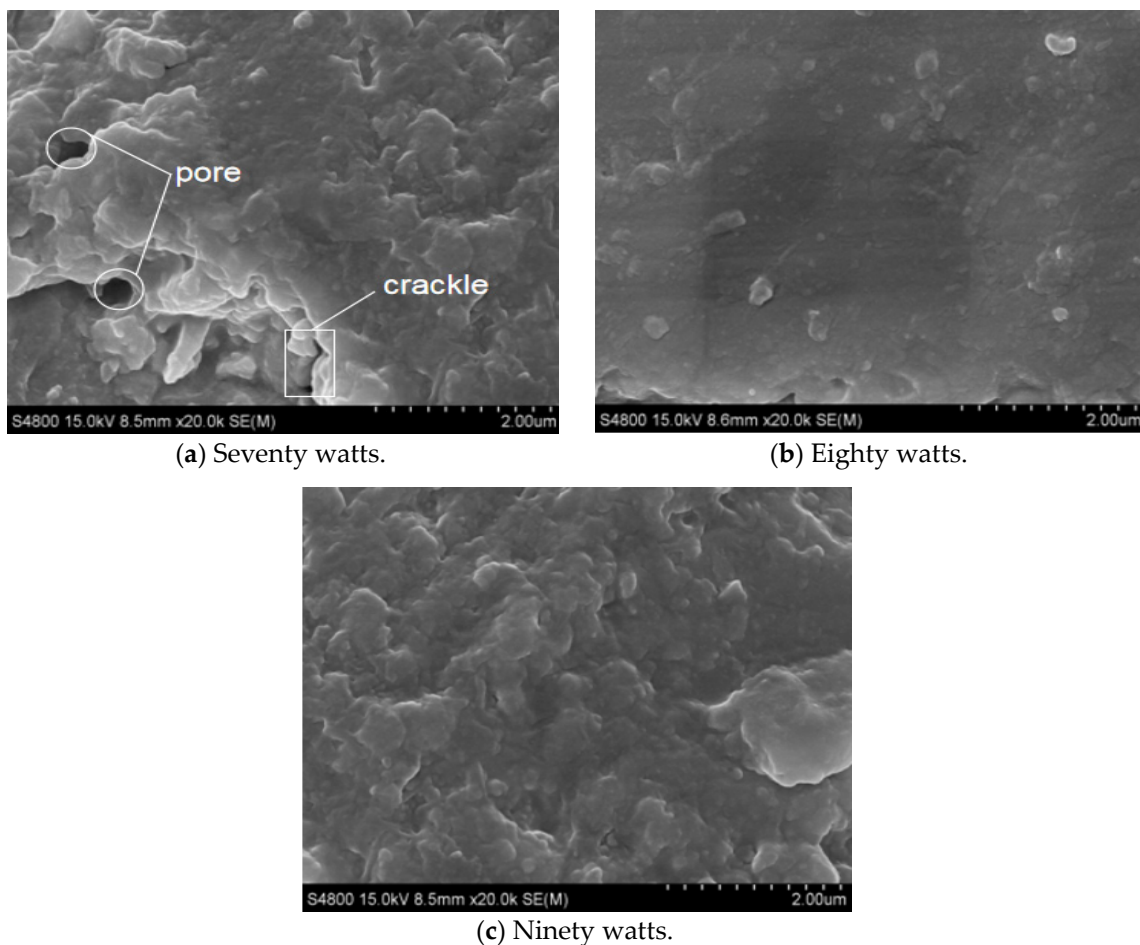


Figure 3. Surface morphology of the laser-sealed layer. (a): Seventy watts; (b): Eighty watts; (c): Ninety watts.

Figure 4 shows the micro morphology under the sealing speed of 1, 2, 3, and 4 mm/s. As shown in Figure 4a, when the sealing speed is 1 mm/s, there are some defects on the surface of the sealing layer, the surface is not smooth enough. There are a few block structures, small holes, and tiny cracks. Because the output energy of the laser per unit time is too large, the viscosity of the molten solder is very low, and it is damaged at a high temperature. With the increase in sealing speed, at 2 mm/s, the block structure, pores, and cracks disappear, and the surface is flat and dense, as shown in Figure 4b. The output energy of laser per unit time decreases, which makes the temperature of the molten solder decrease, without material damage, solder melts completely, and there are almost no solid solder particles in the sealing layer. When the welding speed is 3 and 4 mm/s, there are more blocky structures in the sealing layer, and there are more pores and cracks between the blocky structures. The cracks extend along the edge of the pores. As the energy output per unit of time is further reduced, the solder temperature is not enough to make the solder melt completely.

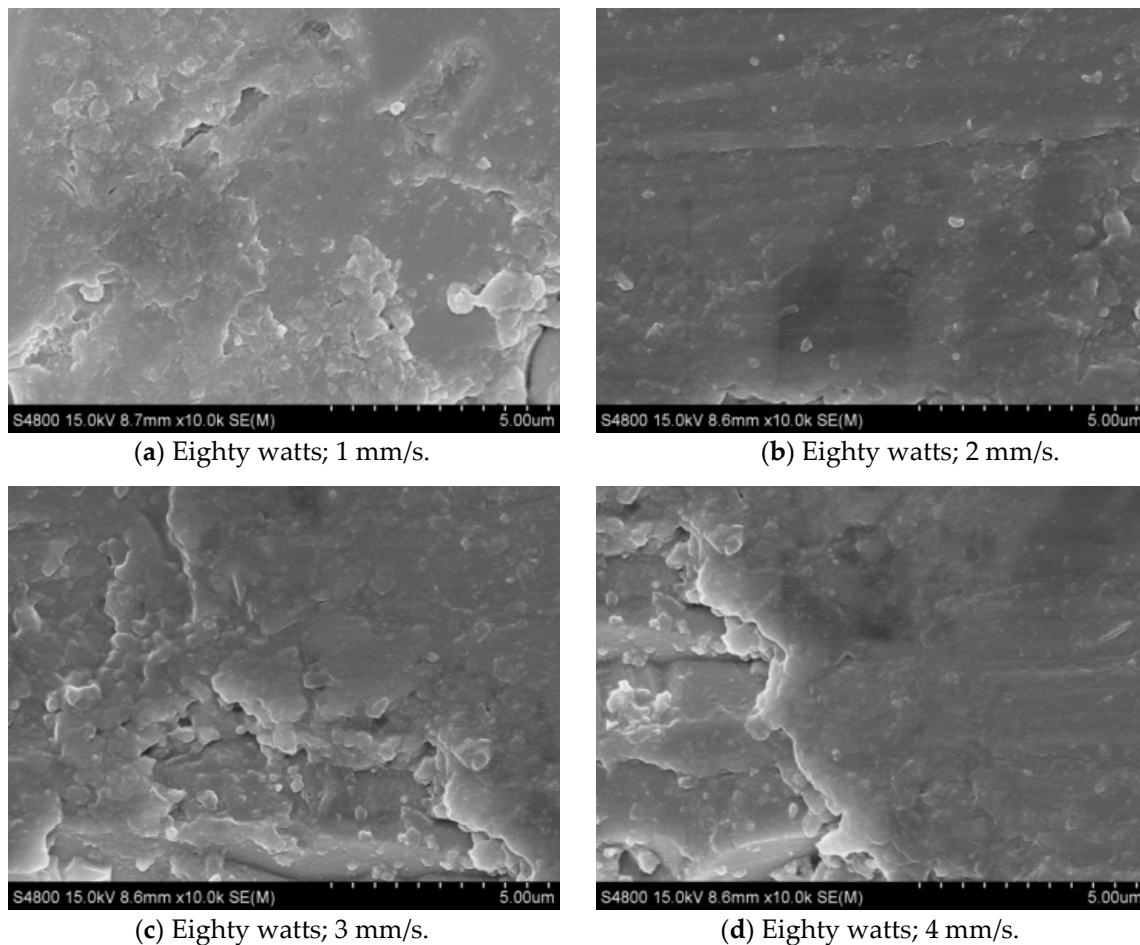


Figure 4. Cross-sectional morphology of bond between solder and glass at different welding speeds. (a): 1 mm/s; (b): 2 mm/s; (c): 3 mm/s; (d): 4 mm/s.

3.2. Crack Formation Analysis with Laser-Sealed Vacuum Glass

When the laser power and sealing speed are not suitable, pores and cracks can easily appear in the sealing layer, and they radiate outward to form microscopic cracks, which have a strong elongation ability. Further analysis of the causes of cracks, including negative expansion solder type selection and solder particle size and distribution, are presented. In the cooling stage after melt densification, due to the different expansion coefficients of the solder and glass matrix, it is difficult to adjust the elastic deformation, which eventually leads to cracks. When the solder particles are small, and the distribution of particles is not uniform or concentrated, it will also form a large stress concentration, even microcrack defects.

Figure 5 shows the results of wetting at different temperatures, the interface between the sealing solder and the glass substrate. There is a hot plate to rise the temperature to 450 and 470 degrees Celsius. At the lower limit temperature (450 °C), it can be seen from Figure 5a, from the micro morphology, that the sealing solder has basically covered the surface of the glass matrix and is closely connected with the glass matrix, but the wettability is not ideal, and there is a clear boundary between the solder and the glass matrix. At the interface between solder and glass matrix, the particle block structure and liquid phase structure coexist, which indicates that the component with a lower melting point in solder at the interface has melted into the liquid phase, showing certain fluidity and filling the "gap" between the solder and glass matrix surface, but the un-melted particle structure hinders the flow of the liquid phase. In Figure 5a, the "river bed" is due to the filling of the liquid phase structure defect formed by voids. When the temperature of the sealing solder rises to 470 °C, it can be seen from Figure 5b that the sealing solder has completely covered the surface of the glass substrate and no

obvious transition zone has been formed. In addition, the solder at the interface is closely connected with the glass matrix without “gap” defects. The results show that when the sintering temperature is increased, the main components of the solder are melted. At this time, the sealing solder should have good fluidity, and the wettability between the sealing solder and the glass substrate surface becomes better. The energy spectrum of transition zone A is tested, as shown in Figure 6. The results show that the atomic number fraction of Si and Pb in zone B is 3.04% and 68.93% respectively, which is higher than that in raw materials. It is concluded that the transition layer is mainly the mixture of PbO and SiO₂, which indicates that PbO and SiO₂ in the solder are more conducive to wetting the glass substrate surface and improving the bonding quality between the solder and the glass substrate.

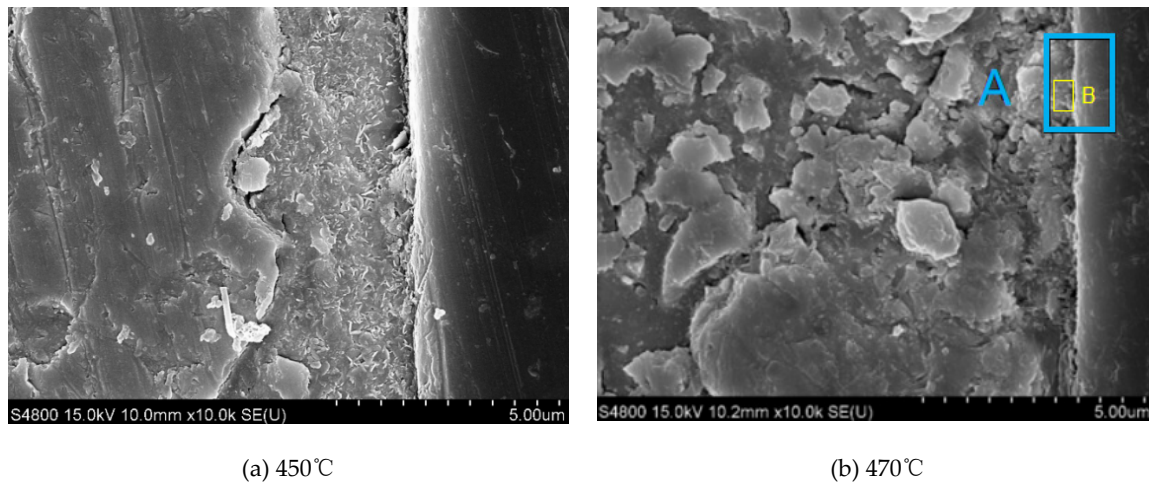


Figure 5. Scanning electron microscopic (SEM) photograph showing the wetting interface between the sealing solder and glass matrix. (a): 450 °C; (b): 470 °C.

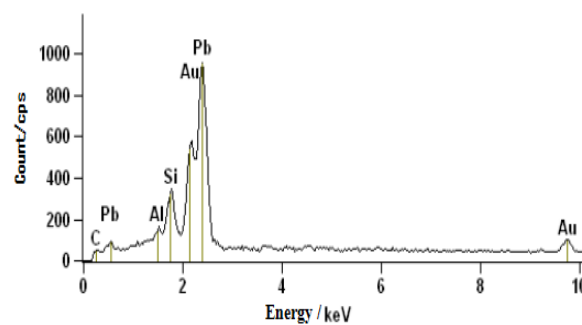


Figure 6. Energy spectrum of the interface between the sealing solder and glass matrix transition layer.

4. Conclusions

The vacuum tightness of the seal is a principal need to achieve the successful vacuum plate glass. Overall, it has been found that a perfect laser seal not only requires solder but an appropriate environment, laser power, sealing speed, and sealing temperatures. In this paper, the pores, cracks, and interface with laser welding are analyzed in depth using PbO-TiO₂-SiO₂-R_xO_y system sealing solder to prepare vacuum flat glass. The microstructure of the sealing layer was analyzed by a BX41M-LED metallographic microscope, and the interfacial bonding characteristics were observed by thermal field emission scanning electron microscopy (SEM). The solder was analyzed by an energy spectrometer and the influence of laser power, sealing temperature, and sealing speed on the gas holes and crack sand interface separation of the sealing layer are reported. With this being taken into account, a range of experiments were conducted to construct vacuum plate glass, and the following conclusions are obtained:

- (i) The smaller the welding speed, the larger the laser power, causing higher surface porosity defects and a larger block structure. When the welding speed increases and the laser energy output per unit time is too high, the solder is vulnerable to burns. Therefore, when the laser power is 80 W and the welding speed is 2 mm/s, the sealing layer has almost no porosity and the quality of the seal achievable is suitable for vacuum-sealed glass.
- (ii) When the welding temperature reaches 470 °C, the interface between solder and glass becomes compact and flat, and the wettability of the interface becomes better. When the welding temperature is too low, the solid–liquid absorption of the sealing layer leads to the obvious phenomenon of interface separation, and the interface between the solder and the glass becomes uneven, and there is a gap on the surface of the sealing layer.
- (iii) The energy spectrum test of the transition layer shows that the solder and the glass matrix wetted layer is closely combined due to the composition of the solder including Si and Pb elements, which reduces the separation phenomenon of the interface of the sealing layer and improves the bonding quality of the solder and the glass matrix.

Author Contributions: Conceptualization, H.M. and S.L.; methodology, validation, S.Z., L.Z.; formal analysis, S.Z., H.M., L.Z., B.Z.; investigation, H.M., S.Z. and S.L.; writing—original draft preparation, H.M., L.Z., S.L., S.Z., B.Z. and S.M.; writing—review and editing, S.M., S.Z., S.L., H.M., B.Z., L.Z., H.M. All authors have read and agreed to the published version of the manuscript.

Funding: This work was supported by National Natural Science Foundation of China (Grant No. 51672241), Natural Science Foundation of Jiangsu Province (No. BK20170500), Natural Science Foundation of the Jiangsu Higher Education Institutions (No. 18KJB460032), 14th batch High-level Talents Project for “Six Talents Peak” (Grant No. XCL-092), Jiangsu Science and Technology Plan Project of China (Grant No. BE2016134), Province Postdoctoral Foundation of Jiangsu (Grant No.1501164B), Technical Innovation Nurturing Foundation of Yangzhou University (Grant No. 2017CXJ021, 2017CXJ024), China Postdoctoral Science Foundation (Grant No. 2016M600447), Yangzhou Foundation Innovation Project (Grant No. YZ2017052, YZ2017279, YZ2017275) and Yangzhou University College student Science Foundation Project (x20180290).

Acknowledgments: This work supported by the National Natural Science Foundation of China, Natural Science Foundation of Jiangsu Province, Technical Innovation Nurturing Foundation of Yangzhou University, China Postdoctoral Science Foundation, Yangzhou University College student Science Foundation Project and London South Bank University. Authors would like to thank the reviewers and editors for their suggestions.

Conflicts of Interest: The authors declare no conflict of interest.

References

1. Fang, Y.; Memon, S.; Peng, J.; Tyrer, M.; Ming, T. Solar thermal performance of two innovative configurations of air-vacuum layered triple glazed windows. *Renew. Energy* **2020**, *150*, 167–175. [[CrossRef](#)]
2. Memon, S.; Fang, Y.; Eames, P.C. The influence of low-temperature surface induction on evacuation, pump-out hole sealing and thermal performance of composite edge-sealed vacuum insulated glazing. *Renew. Energy* **2019**, *135*, 450–464. [[CrossRef](#)]
3. Katsura, T.; Memon, S.; Radwan, A.; Nakamura, M.; Nagano, K. Thermal performance analysis of a new structured-core translucent vacuum insulation panel in comparison to vacuum glazing: Experimental and theoretically validated analyses. *Sol. Energy* **2020**, *199*, 326–346. [[CrossRef](#)]
4. Memon, S.; Eames, P.C. Predicting the solar energy and space-heating energy performance for solid-wall detached house retrofitted with the composite edge-sealed triple vacuum glazing. *Energy Procedia* **2017**, *122*, 565–570. [[CrossRef](#)]
5. Lei, Z.L.; Li, Y.; Chen, Y.B.; Sun, Z.S.; Zhang, Y.K. Effect of double-beam laser filamentation welding process on the porosity of aluminum alloy welding. *J. Weld.* **2013**, *34*, 40–44.
6. Su, S.H.; Yu, Y.L.; Fei, W.; Lin, S.J.; Wu, W.C.; Cao, Y.; Zhang, J.; Tang, X.H. Characteristics of aluminum alloy weld forming in high-power fiber laser welding. *Laser Technol.* **2017**, *41*, 322–327.
7. Wang, X.H.; Gu, X.Y.; Sun, D.Q. Study on the interface characteristics of laser welding joints of steel/aluminum heterogeneous metals. *J. Mech. Eng.* **2017**, *53*, 26–33. [[CrossRef](#)]
8. Hao, X.H.; Ju, Y.L.; Lu, Y.J. Experimental study on the sealing clearance between the labyrinth sealing displacer and cylinder in the 10K G-M refrigerator. *Cryogenics* **2011**, *51*, 203–208. [[CrossRef](#)]

9. Luo, X.L.; Yu, X.J.; Wang, Y.L. Sealing technology of glass and metal in SiO₂—BaO system. *Acta Silic. Sin.* **2013**, *41*, 858–862.
10. Han, M.F.; Du, J.P. Properties of magnesium oxide composite bi₂o₃-bao-sio₂-rxoy glass sealing material. *Acta Silic. Sin.* **2011**, *39*, 1102–1107.
11. Miao, H.; Shan, X.; Zhang, R.H.; Zhang, J.F.; Zuo, D.W.; Wang, H.J. Properties of vacuum plate glass for sealing. *J. Funct. Mater.* **2014**, *21*, 21094–21097, 21102.
12. Zhang, J.; Liu, S.; Zhang, Y.; Miao, H.; Zhang, S.; Zhang, Q. Formation mechanism of sealing edge pores for vacuum glazing using laser brazing technique. *Vacuum* **2017**, *147*, 1–7. [[CrossRef](#)]
13. Zhang, S.; Li, C.; Miao, H.; He, Q. The influence of welding process parameters on the pores formation in pulsed laser-welded vacuum plate glazing. *Materials* **2019**, *12*, 1790. [[CrossRef](#)] [[PubMed](#)]
14. He, Q. *Numerical Simulation and Experimental Study of Laser Sealed Vacuum Flat Glass*; Yangzhou University: Yangzhou, China, 2019.
15. Han, M.F.; Du, J.P. Sealing performance of Bi₂O₃-BaO-SiO₂-R_xO_y glass. *Rare Met. Mater. Eng.* **2011**, *40*, 279–283.
16. Song, Y.Q.; Dong, J.F.; Sun, H.Z. Scanning electron microscopy of insect materials. *Hubei Agric. Sci.* **2013**, *52*, 1064–1065, 1070.
17. Memon, S.; Farukh, F.; Kandan, K. Effect of cavity vacuum pressure diminution on thermal performance of triple vacuum glazing. *Appl. Sci.* **2018**, *8*, 1705. [[CrossRef](#)]
18. Luo, D.W.; Shen, Z.S. Porosity and glass splash during glass and metal sealing. *J. Beijing Univ. Sci. Technol.* **2011**, *33*, 856–862.
19. Zhou, J.X.; Tang, X.H.; Zhou, Y.; He, Y.Y.; Zhu, G.F. Research on stomata phenomenon in laser welding of powder metallurgy materials. *Laser Technol.* **2003**, *27*, 503–505.
20. Kind, H.; Gehlen, E.; Aden, M.; Olowinsky, A.; Gillner, A. Laser Glass Frit Sealing for Encapsulation of Vacuum Insulation Glasses. *Phys. Procedia* **2014**, *56*, 673–680. [[CrossRef](#)]
21. Huang, Y.J. Influence of laser welding parameters on mechanical properties of plexiglass and stainless steel joints. *China Laser* **2017**, *44*, 1202006. [[CrossRef](#)]



© 2020 by the authors. Licensee MDPI, Basel, Switzerland. This article is an open access article distributed under the terms and conditions of the Creative Commons Attribution (CC BY) license (<http://creativecommons.org/licenses/by/4.0/>).